CHALMERS
UNIVERSITY OF TECHNOLOGY

Electrochromic Passive Matrix Display Utilizing Diode-Like Redox Reactions on Indium-Tin-Oxide

Electrochromic Passive Matrix Display Utilizing Diode-Like Redox Reactions on Indium-Tin-Oxide

*Oliver Olsson, Marika Gugole, Jolie C. Blake, Ioannis Petsagkourakis, Peter Andersson Ersman, and Andreas Dahlin**

Recent years have shown many advances in the development of tunable structural colors by combining nanostructures with electrochromic materials. One main goal is to develop energy saving color displays that rely on ambient light instead of being emissive. However, all displays need to be pixelated to show arbitrary images and few studies have addressed the challenge of preparing and controlling individual electrochromic pixels. Herein, a very simple method to reach this milestone by using passive matrix addressing is presented, which requires no additional electronic components in the pixels. It is shown that the common transparent conductor indium tin oxide (ITO) in non-aqueous electrolytes exhibits the diode-like behavior (threshold in voltage in relation to current and coloration) necessary to prevent significant cross-talk between pixels. The chemical nature of the redox activity that enables this behavior is attributed to omnipresent oxygen and the formation of superoxide ions. Additionally, it is shown that a gel-like electrolyte can be prepared by optical lithography, which makes the concept compatible with patterning of pixels at high resolution. This method for preparing pixelated displays should be compatible with practically any type of electrochromic surface in both reflective and transmissive configurations. Also, the counter electrode maintains excellent transparency since it simply consists of ITO. The results should prove very useful as the research field of tunable structural colors moves from proof-of-concept to real devices.

1. Introduction

Electronic displays are becoming more and more frequent in everyday life due to increased digitalization and the internet of things. While almost all existing technologies, in particular light-emitting diodes (LEDs) and backlit liquid crystal displays (LCDs), emit light, there are also displays that rely on ambient light,[1] often referred to as electronic paper.[2] Such displays attract great technical and commercial interest due to their specific advantages, which include extremely low energy consumption and excellent visibility under conditions of strong ambient light (e.g., under the sun). It is challenging, however, to produce electronic paper with good performance in color mode.[2] At the same time, good image quality in color mode is a requirement for certain commercial applications and increases the possibility to highlight different types of information. Recently, the challenge of improving electronic paper in color has been addressed by various combinations of electrochromic materials and structural colors,[3,4] aiming to improve vibrance, brightness (reflectance), and contrast. While several significant advances have been made, including even video speed operation,[5,6] a requirement for a display device to show an arbitrary image is that the display is pixelated (not just segmented) into a 2D matrix with individual pixel addressability. Although a few examples have been presented,[7,8] the question of how to realize pixelated devices with structural colors has been somewhat overlooked. Separate connectors to each pixel is clearly not an option since one wants to preserve a high fill factor of the display area.[4]

Two addressing approaches are possible for realizing pixelated electrochromic devices: active or passive matrix.[4] An active matrix consists of a transistor array, which provides full functionality but requires many fabrication steps.[9,10] Also, it is not obvious how structural colors and electrochromic materials can be easily integrated in pixels including transistors, especially without reducing the fill factor. As an alternative, the passive matrix approach requires no additional electronic components in each pixel and can thus be prepared very easily: two surfaces with electrode stripes are bonded together such that an array of pixels is formed. This fits well in the context of electronic paper technologies where the goal often is to produce simple devices that still provide fair image quality, so that they can replace high-energy consuming emissive displays in (at least some) applications. However, passive matrix approaches often suffer from cross-talk between pixels, i.e., they cannot be fully individually addressed.[11] One requirement for electrochromic devices in a passive matrix configuration is that the electrolyte is not global,

O. Olsson, M. Gugole, J. C. Blake, A. Dahlin
Department of Chemistry and Chemical Engineering
Chalmers University of Technology
41296 Gothenburg, Sweden
E-mail: adahlin@chalmers.se

I. Petsagkourakis, P. Andersson Ersman
Printed, Bio- and Organic Electronics
RISE Research Institutes of Sweden
60233 Norrköping, Sweden

The ORCID identification number(s) for the author(s) of this article can be found under https://doi.org/10.1002/adem.202302141.

DOI: 10.1002/adem.202302141

but patterned just like the pixels.[4] The other main issue is that neighboring pixels, i.e., those that are not to be switched, will always experience a significant voltage. Therefore, the electrochromic material must exhibit an electro-optical response that is insensitive in a certain voltage range. However, thin films of electrochromic materials tend to exhibit continuous changes in optical properties with voltage since it directly determines the degree of doping/intercalation.[3] One way to alter the electro-optical properties of the pixel cells is to use counter electrodes that exhibit threshold behavior in their current–voltage relationship, thereby offering control of the charge transfer required to switch the electrochromic material.[11,12] Additional material coatings may be introduced to create this behavior.[13] However, this imposes limitations on device design because the counter electrode should not be opaque as the observer typically looks through it and the electrolyte.

Examples of pixelated electrochromic devices operated by passive matrix addressing do exist, but are normally based on redox-active dyes in solution phase[14–19] rather than electrochromic surfaces and nanostructures. Redox reactions with solutes normally have intrinsic threshold-like behavior with voltage, while films of electrochromic materials do not. Hence previous work on passive matrix implementation is quite limited for the case of electrochromic surfaces. Recently, Li et al.[7] presented a device based on tungsten trioxide (WO_3) films, but the pixels were switched simply by utilizing the long optical memory of WO_3 and a single row and column was connected for each switch. For the well-studied poly(3,4-ethylenedioxythiophene): poly(4-styrenesulfonate) PEDOT:PSS electrochromic system, passive matrix operation has been demonstrated,[12] even with "grayscale" tuning in screen printed displays.[20] However, those devices (e.g., the Acreo display from the RISE Printed Electronics Arena) use carbon electrodes hidden behind opaque electrolytes and thus they do not present a generic strategy for passive matrix operation of electrochromic surface films and tunable structural colors. Alternatively, PEDOT:PSS can be combined with a ferroelectric material to be used in a passive matrix configuration, but the ferroelectric effect requires voltages of ≈10 V.[21]

In this work, we present a generic and simple strategy for realizing pixelated electrochromic surfaces operating in a passive matrix configuration. We perform a systematic investigation of when and how these devices work. Bare ITO, which remains the ideal as the transparent conductor forming the opposite "window" in devices,[7,22] is shown to give rise to diode-like behavior in stable non-aqueous electrolytes. This effect directly limits charge transfer to the electrochromic surface, thereby enabling passive matrix addressing. Our approach makes it possible to easily produce devices that can be scaled up with parallel patterning techniques. Furthermore, we shed light on the reaction causing the threshold behavior in the current–voltage relation for ITO. Our passive matrix design works for both reflective and transmissive devices and should be highly interesting for pixelation of recently developed electrochromic nanostructures.

2. Results and Discussion

2.1. Material Properties and Requirements

As a theoretical background, we begin by describing the principal requirements on material properties for a given system to work in a passive matrix configuration with m rows and n columns. Central to the understanding is a concept we refer to as the electro-optical response curve (EORC), which shows the optical property of interest (e.g., reflectivity) versus voltage applied across the pixel electrodes (**Figure 1**). The EORC is generated by sweeping the voltage while measuring the optical response in a synchronized manner. Note that the EORC will depend on the sweep rate to some extent, even for a defined set of

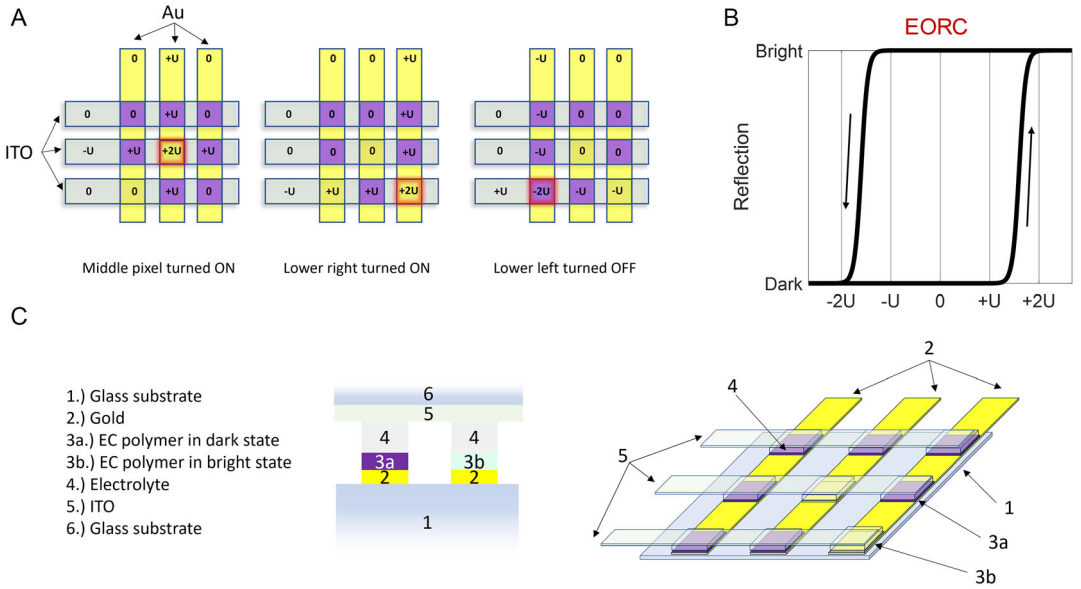

Figure 1. Addressing pixels in a passive matrix. A) Examples of voltages experienced by the addressed versus non-addressed pixels. The pixels should switch at threshold values $\pm 2U$ but not within the interval $\pm U$. B) Principle of the electro-optical response curve (EORC) with the necessary hysteresis. C) Schematic of the device design used in this work.

materials. In our system, only small changes were observed when varying sweep rates from 1 to 1000 m Vs^{-1} (Figure S1, Supporting Information).

The main challenge in passive matrix operation is to minimize the optical response from neighboring pixels, i.e., "cross-talk" effects.[11] Since electrochromic materials exhibit coloration memory, a rudimentary approach is to simply connect to one row and one column to address the pixel of interest, leaving all other rows and columns at open circuit.[7] However, even in this situation the current can flow through neighboring pixels (Figure S2, Supporting Information) and it is not feasible in practice to sequentially connect and disconnect every single row and column to update the image, since such a pixel-by-pixel updating scheme would result in unreasonably slow image update.

As the number of pixels in a display is larger ($m \times n$) than the number of connectors ($m + n$), updating any matrix (active or passive) requires sweeping through all m rows. This, in turn, means that it is not sufficient for the electrochromic material to exhibit a threshold behavior in the EORC because upon addressing the next row, pixels on the previous row will be erased (Figure S3, Supporting Information). However, if the system exhibits hysteresis in the EORC,[20] i.e., one threshold in the direction of positive voltage and another for negative voltages (Figure 1B), the cross-talk can become negligible. Note that the response to an applied voltage is then not explicitly defined but depends on the "history" of previous switching (memory effects). A key point in this work is that even if an electrochromic material has little hysteresis in its EORC, this effect can be induced by the counter electrode in a two-electrode device configuration. Contrary to liquid crystals, who respond to an electric field, electrochromic effects are driven by charge transfer, i.e., the integrated current is directly dictating the optical response (Figure S4, Supporting Information). Therefore, if the counter electrode has diode-like behavior for both voltage polarities, the EORC will show hysteresis even if it is not an intrinsic property of the electrochromic material itself. Interestingly, this corresponds to the complete opposite of the typically desired properties of counter electrodes, which are high charge storage capacity and efficient current delivery to the working electrode in order to ensure that it can switch.[23] We note that one way of blocking current for specific voltages is to introduce diodes into the circuit.[13] However, this is cumbersome since it would require each pixel to have its own diodes and the major advantage of the passive matrix, i.e., its simplicity, is lost. In this work we show that bare "native" ITO exhibits the desired voltage–current behavior in stable electrolytes such as 0.1 M $LiClO_4$ in propylene carbonate (PC).

Another fundamental parameter is the relative areas of the electrodes. In this work we prepare devices where the counter electrode area is the same as the electrochromic surface area, which is obviously the most straightforward design for pixelated displays with high fill factor. However, it should be noted that if the counter electrode area is much larger than that of the electrochromic surface, sufficient charge to switch the electrochromic material may be provided simply from the double layer capacitance. In this case the hysteresis in the EORC becomes much lower, as expected (Figure S5, Supporting Information).

Finally, it should be noted that there are different voltage schemes for passive matrix operation. In Figure 1A, the row and columns to be switched have voltage $\pm U$, while others are set to zero potential, but this is just an example. Another option is different versions of the $U/3$ scheme.[12,20] The most suitable protocol may depend on the shape of the EORC curve.

2.2. ITO as Counter Electrode Directly Enables Passive Matrix Displays

Throughout this work, unless otherwise specified, we use simple electrochromic surfaces consisting of polydimethylpropylenedioxythiophene ($PProDOTMe_2$) on 100 nm gold and measure the reflection of light. We have previously characterized this system thoroughly in conventional three-electrode systems and $PProDOTMe_2$ is known for its excellent switching contrast[24] and response time.[5] Note, however, that the devices presented here are not necessarily optimized with respect to these parameters since the purpose is to investigate passive matrix operation. The films were electropolymerized to a charge transfer of around 10 mC cm^{-2}, corresponding to ≈75 nm thickness and a power consumption per switch of ≈1 mJcm^{-2}.[24] Importantly, planar gold surfaces were used because of their simplicity, but the gold film can easily be replaced with practically any kind of metasurface exhibiting structural colors. Indeed, many have gold as the top material.[5,24–27] Similarly, one should be able to use practically any electrochromic material, organic, or inorganic.

Figure 2A shows the characteristic EORC curve (reflectivity plotted at 630 nm) generated with a conventional three-electrode setup. The optical response saturates in both directions because the polymer film is fully doped/undoped at sufficiently high/low potentials. Note that the hysteresis is minimal in this case. This is because the sweep rate is slow enough for the polymer to essentially fully equilibrate its doping degree at each potential, which is measured against a stable reference electrode in the three-electrode configuration.

To prepare a complete device, we used planar ITO as a simple transparent counter (and reference) electrode through which the electrochromic surface is to be viewed. Strikingly, this had a major impact on the EORC curve, which started to exhibit clear hysteresis (Figure 2A). This effect occurred in a simple electrolyte consisting of $LiClO_4$ in PC without any redox active species added. To verify that the hysteresis in the EORC was a direct consequence of the ITO electrode limiting charge transfer to the electrochromic material in a certain potential window, we checked the cyclic voltammetry (CV) curves of ITO in a three-electrode setup (Figure 2B). This means that ITO is the working electrode (WE), while the reference electrode (RE) is Ag/Ag^+ and the counter electrode (CE) is Pt. Indeed, high currents were only generated after a certain threshold potential had been reached, in both sweep directions (around −1 and +1 V vs Ag/Ag^+). When performing CV on $PProDOTMe_2$ on gold, the curve goes from the expected shape in the three-electrode configuration to peak separation when in a two-electrode configuration with ITO as CE (and RE). As a final verification, we also measured (passively) the voltage between the gold with the electrochromic polymer and an Ag/Ag^+ electrode while switching in the two-electrode

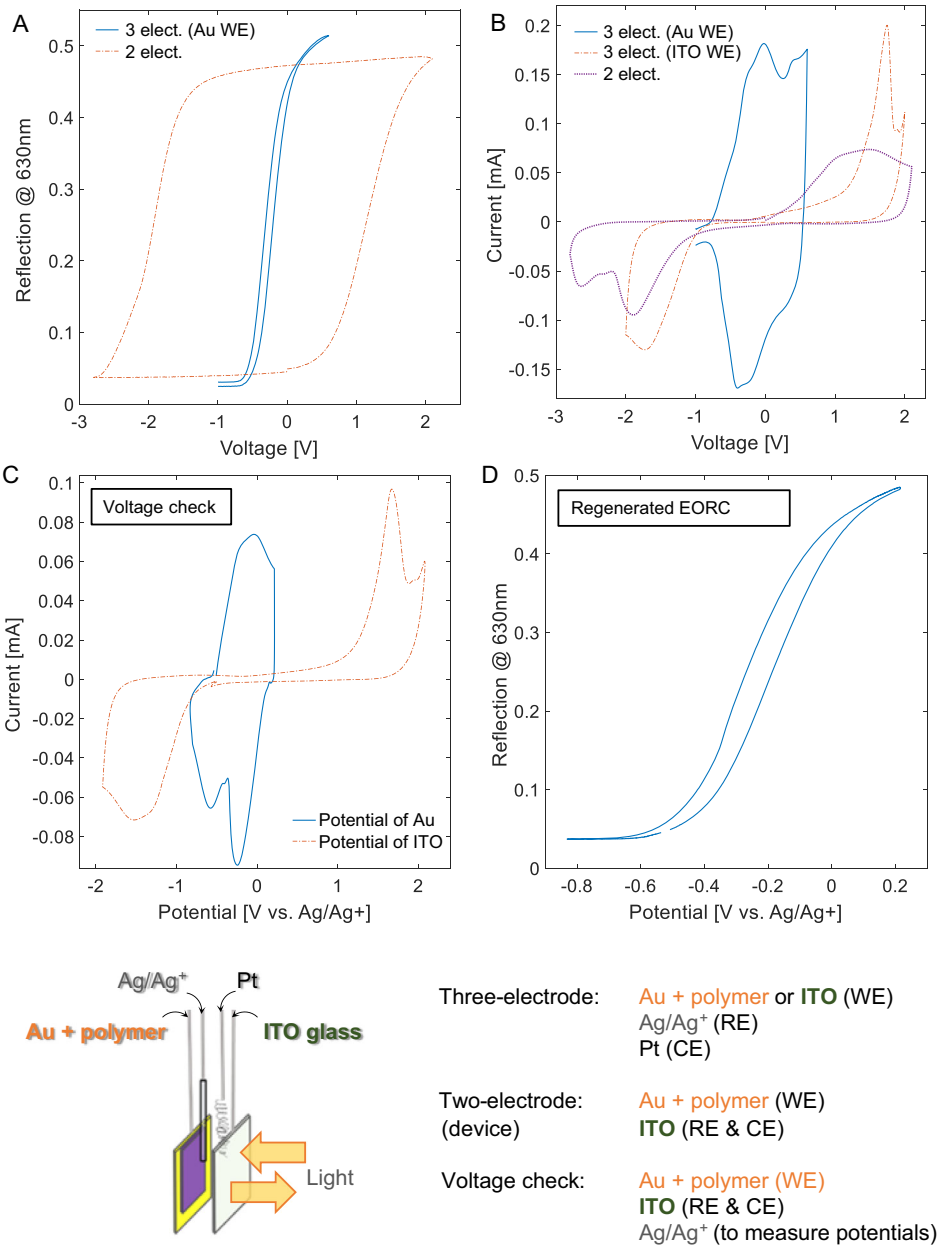

Figure 2. Diode-like behavior of ITO gives rise to hysteresis in the electro-optical response. A) EORC for the electrochromic surface (gold and polymer) in a three-electrode setup (Ag/Ag^+ reference and Pt counter) versus the two-electrode device configuration (ITO as combined reference and counter). B) CV scans of the polymer on gold (solid line) or pure ITO (dashed), both in the three-electrode configuration. A CV scan when using the two-electrode configuration is also shown (dotted). C) Control experiment using the two-electrode configuration with additional passive measurements of electrode potential versus Ag/Ag^+. (Note that the curves look similar in shape to those in panel (B)). D) EORC generated for gold with polymer from the potential values in panel C (vs. Ag/Ag^+). (Note that the curve looks similar to that in panel (A)). The scan rate was 100 mV s^{-1} in all cases.

configuration.[28] This made it possible to construct the expected CV curves for the three-electrode configuration (Figure 2C), which were indeed very similar to those actually measured (Figure 2B). (The current is lower because the effective scan rate is slower.) Based on the measured potentials versus Ag/Ag^+, an EORC could also be generated (Figure 2D) which looked similar to the one from the three-electrode configuration (Figure 2A). These experiments show that the hysteresis is not representing a change in the electrochromic properties of the gold electrodes, i.e., the behavior of $PProDOTMe_2$ versus applied voltage is unchanged, as expected since the polymer electrode is the same. However, in the two-electrode configuration its capability to switch becomes strongly influenced by the diode-like behavior of ITO. This, in turn, strongly suggests that the method we use is generic and should be applicable to other electrochromic materials as well.

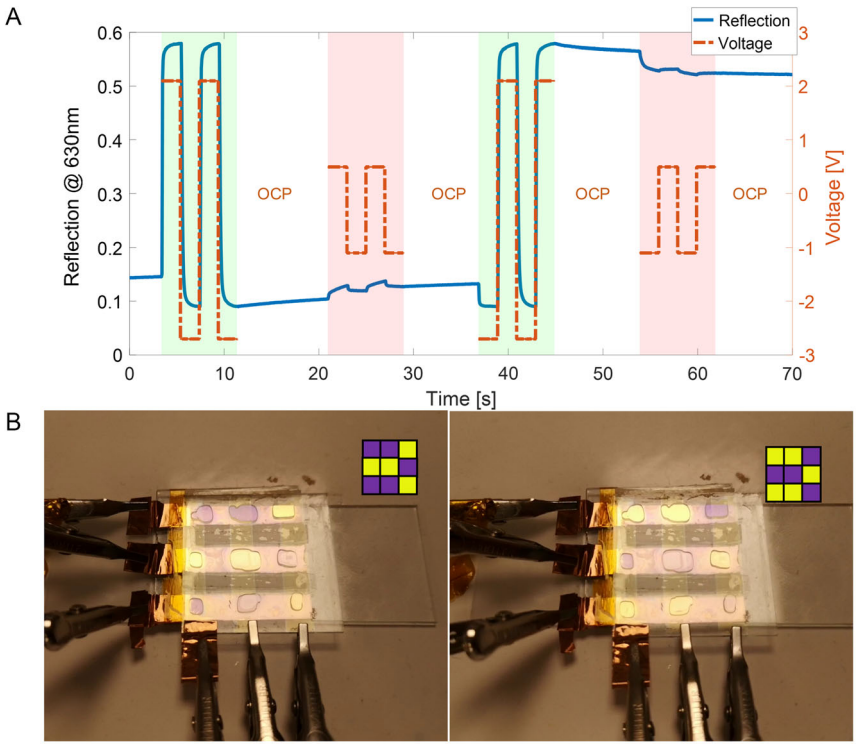

Figure 3. Device performance. A) Optical response from the electrochromic surface when exposed to different voltages versus ITO in the two-electrode configuration. The voltages represent either those in addressed pixels, i.e., −2.7 V for "on" (purple) or +2.1 V for "off" (goldish), or those in non-addressed pixels (+0.5 or −1.1 V). OCP means open circuit voltage. B) Photos of a 3 × 3 pixelated device which inverts its pattern according to the insets.

We verified that the cross-talk voltages would not give a significant electrochromic response by applying them in the two electrode device configuration (**Figure 3**A). Even after several seconds, the optical response from the voltages that would be applied to pixels that are not to be switched (Figure S6, Supporting Information) was <10% of the response from the "correct" switching voltage. As proof of concept, Figure 3B shows a complete 3 × 3 passive matrix device fabricated by simple stripes of gold and ITO electrodes which are aligned perpendicularly and bonded together with double sided tape. Each intersection of two stripes creates a pixel which becomes a separate electrochemical cell. The device is programmed to display a certain pattern which is then successfully inversed, i.e., each dark pixel becomes bright and vice versa. The supporting information contains a video showing the pixel updating in real-time (Video S1, Supporting Information). For these test devices, each pixel was addressed in series for ≈100 ms, which makes the complete change to the other image state relatively slow (>1 s). In a real device all pixels in a row could be addressed in parallel which greatly reduced the time required to update the full image. As expected, individual pixels in devices showed the same threshold behavior in the voltage–current curves as measured on macroscopic surfaces (not shown).

2.3. Mechanism Underlying Diode-Like Behavior of ITO

With its high conductivity and transparency in the visible spectra, ITO, often together with an ion-storage layer,[23] is established as a suitable counter electrode material in electrochromic devices.[22] However, hysteresis in the EORC appears to never have been explicitly reported or systematically investigated, although it is the central property for enabling passive matrix operation. Instead, much effort has been spent on modifying ITO to increase the charge storage capacity without sacrificing transparency. Our approach in this work requires exactly the opposite: the counter electrode should have limited capacitance so that its diode-like redox activity dictates charge transfer to the electrochromic material. In this section we elucidate the chemical nature of the mechanism causing the threshold voltage behavior in the CV curves.

Previous studies have investigated the electrochemical activity of ITO which appears below −2.0 V versus Ag/Ag^+ in electrolytes containing Li^+.[22,28–30] These current peaks have been considered to be intercalation of lithium into the ITO,[29,31] although no real consensus has yet been reached.[32,33] We also observed this effect and could generally confirm reactions involving Li^+ by varying the electrolyte composition. However, even though this reaction could potentially be utilized to generate diode-like behavior, we found that it reduced the hysteresis in the EORC (Figure S7, Supporting Information), which makes it detrimental to passive matrix operation. Therefore, we let our devices operate in a potential range above −2.0 V versus Ag/Ag^+. In this case, the diode-like behavior of the ITO electrode was not due to direct reactions with Li^+ because the electrolyte concentration no longer had a strong effect on the currents measured (Figure S8, Supporting Information).

To further investigate the nature of the reaction, we performed more CV experiments on bare ITO using the ordinary three-electrode configuration. We noted that the anodic peak was much stronger if there had first been a cathodic polarization sweep (**Figure 4**A). This suggests that a species formed at cathodic potentials is responsible for much of the redox activity at anodic potentials. Furthermore, a series of sweeps in the direction of negative voltage produced less current every time, while repeated sweeps only towards positive voltages looked the same (Figure 4B). This strongly suggests that at negative potentials, a surface coating is formed that passivates the electrode, but it can be oxidized again at positive potentials so that the ITO is regenerated. Indeed, after performing several cathodic sweeps, surface properties such as contact angle were noticeably changed. To get a direct confirmation of surface precipitation, a quartz crystal microbalance (QCM) with electrochemistry was used. A strong decrease in the resonance frequency was observed after cathodic polarization (Figure 4C). This means that reduction of indium or tin in ITO,[28] i.e., lower oxygen content in the film, cannot occur to any high extent since it would lead to a mass loss, i.e., the opposite of what the QCM data shows. The baseline could be recovered after subsequent anodic polarization (Figure 4D), showing that the material on the surface is dissolved again. Note, however, that for the QCM crystals we had to prepare ITO films by another method.[34] Overall, we found that ITO films prepared in different ways or purchased from different manufacturers showed slightly different voltages (vs. Ag/Ag^+) for the onset of current, but the diode-like behavior was observed in all cases and also on fluorine-doped tin oxide (FTO, Figure S9, Supporting Information), consistent with our interpretation that indium reduction does not take place to any high extent. For the QCM experiments, the fact that the reference electrode was slightly different (a simple Ag wire) may also influence the exact onset potential.

Next, we tried to identify what chemical species caused the cathodic precipitation reaction. It is well-known that PC itself is inert, but always contains trace amounts of O_2 and H_2O taken up from ambient air. **Figure 5** shows CVs in PC electrolytes that were prepared in a glovebox to minimize water content (measured ≈100 ppm). Pure N_2 or O_2 was then bubbled through the PC until saturation. Importantly, for N_2 the redox activity is strongly reduced in the potential window used, while it appears very clearly for the case of O_2, which proves its involvement. Note that in all other experiments we did not deliberately add O_2, it was simply spontaneously taken up by PC from ambient air and this is apparently sufficient to create the diode-like behavior.

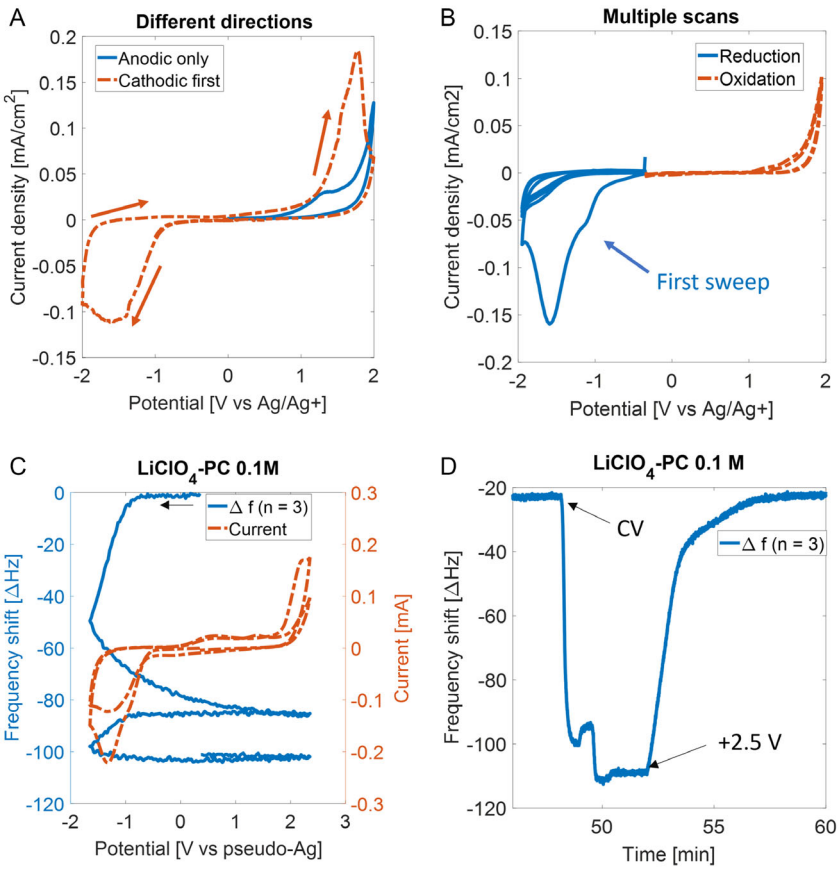

Figure 4. Cathodic redox activity causes surface precipitation and is required for high anodic activity. A) Comparison of currents when performing anodic sweeps with or without first performing a cathodic sweep. B) Multiple sweeps in either the cathodic or the anodic direction. C) Electrochemical QCM response showing surface precipitation during voltages below −1.0 V versus Ag/Ag^+. D) Example of frequency shift vs time upon CV scans and a high positive potential that removes the surface coating. The sweep rate was 100 mV s^{-1} in all plots.

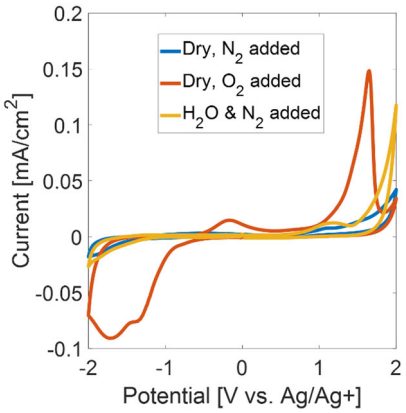

Figure 5. Oxygen is the main cause of cathodic redox activity. CV scans (three-electrode setup) in an electrolyte with minimal water and exposed to only N_2 reduces the current. Introducing O_2 gives the diode-like behavior, while introducing H_2O (8000 ppm) only gives some redox activity at anodic potentials in the range investigated. The sweep rate is 100 mV s^{-1} for all curves.

For comparison, we also measured CVs for an electrolyte where water was deliberately added (8000 ppm). Although some water splitting reactions could be observed, it was mainly for the anodic sweeps and there was no peak in the current as for the case of O_2 (Figure 5). Hence, although H_2O may to some extent contribute to the diode-like behavior of ITO, O_2 is clearly more important.

Based on the aforementioned results, we conclude that the main redox reaction causing the diode-like behavior and the surface coating is associated with reduction of O_2. Most likely, the initial species formed is the superoxide ion:[35]

$$O_2 + e^- \rightleftarrows O_2^- \quad (1)$$

The superoxide ion is known for being relatively long lived and may eventually react with water[36] or PC.[37] However, in the presence of 0.1 M $LiClO_4$ reactions with Li^+ and formation of Li oxides is possible. One example of such a reaction is:[35]

$$O_2^- + Li^+ \rightarrow LiO_2 \quad (2)$$

Thus, we propose that it is a thin layer of lithium and oxygen containing species that precipitate on the surface, just like in lithium-air batteries.[38] The layer is then removed at oxidative potentials.[39] Note that according to this suggested mechanism, ITO itself does not participate in the reaction in the chemical sense.

For comparison, we also tested an electrolyte consisting of tetrabutylammonium perchlorate (TBAP) to alter the cation. The diode-like behavior was observed in this case as well, but electrochemical QCM showed no precipitation on the surface (Figure S10, Supporting Information). In this case the superoxide may react with TBAP, but the product remains in solution phase.[40] Alternatively, the superoxide ion becomes, at least to some extent, oxidized again in the anodic sweep. Similarly, the diode-like behavior also appeared in acetonitrile instead of PC (Figure S11, Supporting Information), which further confirms that it is not the solvent itself which is causing the electrochemical activity.

We emphasize that based on the large number of control experiments in different electrolyte environments, we conclude that the redox activity which we utilize is not caused by any reaction that involves the electrode itself. Yet, the diode-like behavior is still a property of ITO and similar materials such as FTO (Figure S9, Supporting Information) as it was not observed on metallic electrodes. Tests with bare Au and Pt electrodes seemed to exhibit similar reactions, based on similar CV curves, but the large peak separation in the CV curves was diminished (Figure S12, Supporting Information). Furthermore, the increase in peak separation is not solely due to the higher resistance of ITO contra metallic electrodes. By adding resistors in series with the ITO working electrode, a reduction in currents could be observed (Figure S13, Supporting Information), but the threshold voltages were the same.

2.4. Improving Device Design

In this section, we show some additional results that are critical for successful design of future pixelated electrochromic devices based on passive matrix operation with ITO. Since it is straightforward to prepare microscale stripes of electrodes with structural colors by standard optical lithography,[24] the main fabrication challenge for a passive matrix device is that the electrolyte also needs to be patterned into pixels. Hence, electrolytes that can be cured into a gel state by exposure to UV light are highly desirable.[41] We present an example of this in **Figure 6**, which shows how a square-shaped electrolyte has been created by exposure to UV light in this region through a mask. After solidification, chemicals remaining in regions not exposed to UV light were washed away and the sample dried. Note that the surrounding area contains $PProDOTMe_2$ but does not switch since it is no longer in contact with an electrolyte. The electrolyte used for patterning contained poly(ethylene glycol) with acrylate end groups (PEG-DA) that were activated by UV light and 2,2-dimethoxy-2-phenyl-acetophenone[42] (DMPAP). A video showing switching of a device with square-shaped UV-patterned pixels is shown in Video S2, Supporting Information. This shows that fabrication with extremely high pixel density should be possible, limited only by the resolution of UV lithography (≈1 μm). However, a spacer region between pixels is needed for isolation,[19] which will influence the fill factor negatively for very small pixels.

Alternatively, devices can be fabricated by using printing techniques. Screen printing is a relatively rough manufacturing technique, but has nevertheless been used for large-area production of advanced electrochromic displays based on various conducting polymers.[20,43] Herein, the electrolyte ink formulation used for this purpose was based on polyvinylidene fluoride (PVDF). Figure S14, Supporting Information, describes the screen-printing process of the electrolyte in further detail. Although screen-printing can be very fast and simple, UV-based lithography provides the best resolution. Indeed, Gu et al. just showed devices with a fill factor of 89% by UV patterning of electrolyte cells[19] (with dyes in solution generating the electrochromism). The switching capability of the polymer, which is already on the surface during processing, is clearly not

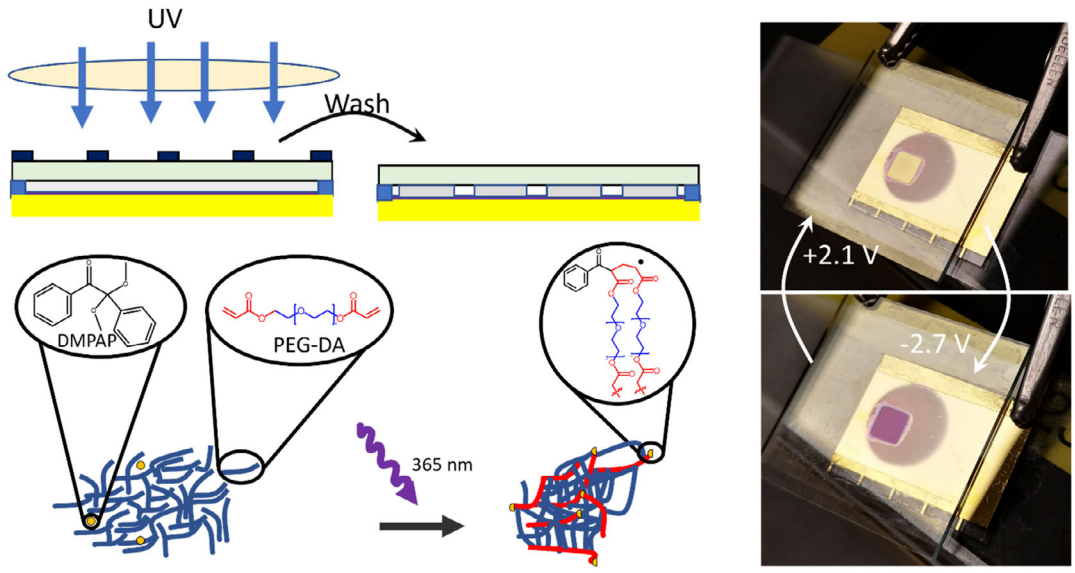

Figure 6. Preparation of electrolyte cells by UV curing. The square shaped region switches because here the gel electrolyte connects the polymer on gold with the ITO. The surrounding grey region contains the polymer (and is therefore dark) but cannot switch because the electrolyte has been washed away (since it was never exposed to UV light).

influenced by the UV lithography (Figure 6) or the screen-printing (Figure S14, Supporting Information).

Besides reflective displays, it may also be of interest to make transparent devices.[15] Such a configuration can be used for placement on windows or for augmented reality. This can be achieved simply by using ITO stripes for both the counter and working electrodes. The diode-like behavior is evident in this case as well, as shown by the EORC which now has transmission on the *y*-axis instead (**Figure 7**A). The relative changes in the optical response from the voltages that would be applied to non-addressed pixels were slightly larger than for the reflective devices (Figure 7B). This is likely related to the polymer thickness which was doubled for devices in the transmission configuration.[24]

A final consideration is the device lifetime. While we did not perform a systematic investigation on this, we used multiple CV curves of ITO as a guideline. (The devices are operated by pulses rather than CV scans, but the latter provides a more informative way to test lifetime.) No significant changes in the threshold behavior of the current response were observed after 10 cycles. After approximately 100 cycles the threshold behavior remained, but the currents at either polarity were reduced in magnitude. The threshold voltage behavior started to disappear around ≈700 cycles (Figure S15, Supporting Information). The loss in optical contrast was typically ≈30% after 100 cycles. It is not clear at this stage what is limiting the lifetime and how much it can be improved. For comparison, although certain devices can switch for over one million cycles,[5] other new switching mechanisms lead to degradation after just a few cycles,[44] which makes us conclude that our lifetime is fairly promising for an initial study. Tentatively, although it is barely detectable in the voltage interval we use (Figure S8, Supporting Information), the Li^+ intercalation

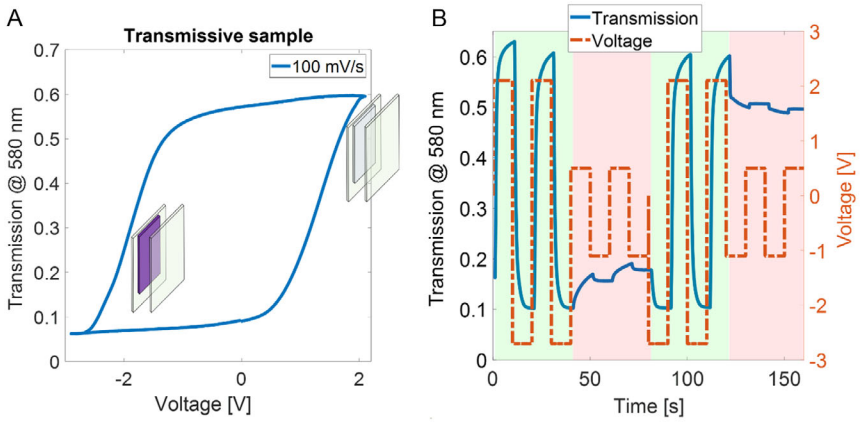

Figure 7. Performance of a transparent device where the two electrodes are ITO with $PProDOTMe_2$ and bare ITO. Instead of monitoring reflection at 630 nm, the transmission at 580 nm is measured. A) Optical response versus voltage (EORC). B) Optical response versus time.

reaction[31] may not be possible to avoid entirely (even when stopping at −2.0 V) and may cause device failure after very many cycles. This suggests that lifetime could be further improved by further investigating different electrolytes. Additionally, minimizing water uptake from ambient air by the electrolyte is critical.[28]

3. Conclusion

We have performed a systematic study to investigate the use of ordinary ITO electrodes for making pixelated electrochromic devices operated via passive matrix addressing protocols. The main advantage of this approach (compared to an active matrix) is that devices become extremely simple to manufacture. An ion storage layer is unnecessary and even detrimental to the performance. Both reflective and transparent display devices can be made. One technical challenge is that the electrolyte also needs to be patterned into pixels, but we have shown that this is possible by UV curing through a photomask, proving compatibility with large scale parallel fabrication. The passive matrix operation with minor cross-talk is possible thanks to the diode-like behavior of ITO, which limits the charge transfer to the electrochromic material unless a threshold voltage is reached, for both polarities. Based on a large number of control experiments, we conclude that the chemical nature of the reaction which enables passive matrix operation is related to dissolved oxygen. Most likely, superoxide ions are formed which react with Li^+ and form a surface coating of LiO_2 (or other oxides) when a threshold voltage is reached in the reductive potential range. While we could detect surface precipitation, we could not achieve consistent and direct experimental evidence of Li species on the surface. (This is not surprising due to the low cross section of Li in X-ray photoelectron spectroscopy.) Regardless of the chemical composition of the film, it is oxidized and dissolved again at another threshold in the positive potential range.

Although the passive matrix design described here has many attractive features, there are also limitations. One important consideration is the time it will take to fully update a device with many pixel rows and whether the diode-like behavior is strong enough to prevent undesired coloration in unaddressed rows. Even a voltage which is too small in amplitude to switch a pixel according to the EORC may still do so if the potential is applied for a very long time. As each row will only be addressed for a fraction $1/m$ of the time, most of the time it will have to withstand the cross-talk voltages without pixels switching. It is important to note that this device ability, which has been referred to as "short-circuit memory" by Beni,[11] will be determined solely by the properties of ITO. Furthermore, it should not be confused with coloration memory, which is a property of the electrochromic material that applies to open circuit conditions.[24] If the current is not zero when a voltage is applied in the interval between the threshold values, it means that some charge is transferred between the electrodes and the electrochromic material will then eventually give rise to a detectable optical response. (Actually, this is indicated by the intensity time trace in Figure 3A, which seems to have small and slow drifts at the cross-talk voltages.) In other words, the hysteresis in the EORC could disappear for an infinitely slow sweep rate. When addressing a row, voltages should therefore ideally be applied to the columns for a duration sufficient to switch the electrochromic material, but not more. This, in turn, means that the switch time of the electrochromic material becomes important for arrays with many pixels and may directly determine how many rows can be included in practice. Thus, passive matrix operation is likely suitable for organic electrochromism where switching can be made fast,[5,6,20] but could be more challenging to get to work with inorganic electrochromic materials, which typically switch an order of magnitude slower.[24]

4. Experimental Section

Chemicals: Propylene carbonate (PC, ReagentPlus 99%), $LiClO_4$ (electrochemical grade), PEG-DA, and DMPAP were purchased from Sigma-Aldrich. TBAP (for electrochemical analysis, ≥99.0%) was purchased from Supelco. Water content was adjusted with MilliQ and determined by Karl-Fischer titration (Mettler Toledo, C20S).

Electrode Surfaces: Glass slides with 100 nm ITO (3×3 cm^2) were purchased from Naranjo Substrates. To make simple electrochromic model surfaces, 100 nm Au (with 1 nm Cr adhesion) was deposited by evaporation (Lesker PVD 225) onto glass slides. $PProDOTMe_2$ was electropolymerized as described previously[24] with sweeps at 100 mV s^{-1}. When depositing on ITO the anodic potential was increased to +1.5 V versus Ag/Ag^+ to yield a uniform film. For EQCMD, ITO coatings were prepared by vacuum deposition and annealing[34] on standard gold sensor crystals (QuartzPro).

Electro-Optical Measurements: Oxygen-free measurements were performed in a closed beaker with a Pt-net and Ag/Ag^+ (Ag in contact with 0.01 M $AgNO_3$ and 0.1 M TBAP) reference electrode (RedoxMe). A Gamry Reference 600+ was used with a custom-made sequence that let the AUX-port act as a separate voltmeter. To control oxygen and water content, the dry electrolyte was degassed with nitrogen and the setup was assembled with a steady flow of nitrogen above the surface. When oxygen was desired the nitrogen line was exchanged for oxygen (99.5%) and bubbled through the electrolyte for 20 min. The pixelated devices were driven by an Arduino interfaced with a LabVIEW program. Measurements of electrochromic surfaces during switching were performed in a home-built microscopy setup for reflection/transmission as described previously.[24]

Photopatterning: A composition of electrolyte as plasticizer and PEG-DA as cross-linker were mixed together with the photoinitiator (DMPAP) in a vial and mixed in a sonicator. The pattern was printed on a transparent plastic paper (OH-film) with a laser printer. A commercial UV-oven was used with a wavelength of 365 nm. To "collimate" the light, the oven was placed 50 cm above the sample and a tube was used to limit the exposure area. 10 min of curing was sufficient to solidify the electrolyte.

Screen Printing: A composition of the electrolyte was made by mixing PC, PVDF:TrFE and salt ($LiClO_4$ or TBAP) in a ratio of 8:2:0.08 g. The ink was stirred under thermal annealing (100 °C) for 60 min and then mixed again using a SpeedMixer DAC (Hauschild). The electrochromic pixel was assembled by screen printing the electrolyte ink on the $Au/PProDOTMe_2$ and bare ITO substrates separately. The electrolyte was then screen printed by hand using a 140-31 polyester mesh on the target substrates, followed by subsequent annealing (100 °C for 15 min and 70 °C for 3 min). Then the two components were pressed together, bringing the electrolyte surfaces in contact to form the electrochromic pixels shown in Figure S14, Supporting Information.

Supporting Information

Supporting Information is available from the Wiley Online Library or from the author.

Acknowledgements

This work was financed by the Swedish Foundation for Strategic Research (EM16-0002). The authors thank Prof. Elisabeth Ahlberg and Assoc. Prof. Per Rudqvist for useful discussions. Eduardo Maurina Morais is acknowledged for help with electrolyte preparation. This work was performed in part at MyFab Chalmers.

Conflict of Interest

The authors declare no conflict of interest.

Data Availability Statement

The data that support the findings of this study are available from the corresponding author upon reasonable request.

Keywords

electrochromism, electronic paper, indium tin oxide, passive matrix, pixels

Received: December 18, 2023
Revised: February 16, 2024
Published online:

[1] K. Xiong, D. Tordera, M. P. Jonsson, A. B. Dahlin, *Rep. Prog. Phys.* **2019**, *82*, 024501.
[2] J. Heikenfeld, P. Drzaic, J.-S. Yeo, T. Koch, *J. Soc. Inf. Disp.* **2011**, *19*, 129.
[3] Y. Kim, C. W. Moon, I. S. Kim, J. Hyun, *Chem. Commun.* **2022**, *58*, 12014.
[4] C. Gu, A.-B. Jia, Y.-M. Zhang, S. X.-A. Zhang, *Chem. Rev.* **2022**, *122*, 14679.
[5] K. Xiong, O. Olsson, J. Svirelis, C. Palasingh, J. Baumberg, A. Dahlin, *Adv. Mater.* **2021**, *33*, 2103217.
[6] K. Xiong, O. Olsson, S. Rossi, G. Wang, M. P. Jonsson, A. Dahlin, J. J. Baumberg, *Adv. Mater.* **2023**, *35*, 2302028.
[7] Y. Li, P. Sun, J. Chen, X. Zha, X. Tang, Z. Chen, Y. Zhang, S. Cong, F. Geng, Z. Zhao, *Adv. Mater.* **2023**, *35*, 2300116.
[8] D. Franklin, Z. He, P. Mastranzo Ortega, A. Safaei, P. Cencillo-Abad, S.-T. Wu, D. Chanda, *Proc. Natl. Acad. Sci.* **2020**, *117*, 13350.
[9] P. Andersson, R. Forchheimer, P. Tehrani, M. Berggren, *Adv. Funct. Mater.* **2007**, *17*, 3074.
[10] B. Bao, B. Rivkin, F. Akbar, D. D. Karnaushenko, V. K. Bandari, L. Teuerle, C. Becker, S. Baunack, D. Karnaushenko, O. G. Schmidt, *Adv. Mater.* **2021**, *33*, 2101272.
[11] G. Beni, L. M. Schiavone, *Appl. Phys. Lett.* **1981**, *38*, 593.
[12] P. Andersson Ersman, J. Kawahara, M. Berggren, *Org. Electron.* **2013**, *14*, 3371.
[13] A. E. Aliev, H. W. Shin, *Displays* **2002**, *23*, 239.
[14] N. Leventis, M. Chen, A. I. Liapis, J. W. Johnson, A. Jain, *J. Electrochem. Soc.* **1998**, *145*, L55.
[15] Y. Wang, S. Wang, X. Wang, W. Zhang, W. Zheng, Y.-M. Zhang, S. X.-A. Zhang, *Nat. Mater.* **2019**, *18*, 1335.
[16] W. Weng, T. Higuchi, M. Suzuki, T. Fukuoka, T. Shimomura, M. Ono, L. Radhakrishnan, H. Wang, N. Suzuki, H. Oveisi, Y. Yamauchi, *Angew. Chem., Int. Edit.* **2010**, *49*, 3956.
[17] M. O. M. Edwards, *Appl. Phys. Lett.* **2005**, *86*, 073507.
[18] N. Kobayashi, S. Miura, M. Nishimura, H. Urano, *Sol. Energy Mater. Sol. Cells* **2008**, *92*, 136.
[19] C. Gu, Y. Yan, J. He, D. Pu, L. Chen, Y.-M. Zhang, S. X.-A. Zhang, *Device* **2023**, *1*, 100126.
[20] P. Andersson Ersman, K. Freitag, J. Kawahara, J. Ahlin, *Sci. Rep.* **2022**, *12*, 10959.
[21] S. Fabiano, N. Sani, J. Kawahara, L. Kergoat, J. Nissa, I. Engquist, X. Crispin, M. Berggren, *Sci. Adv.* **2017**, *3*, e1700345.
[22] D. E. Shen, D. B. Iyer, A. M. Dejneka, J. R. Reynolds, A. M. Osterholm, *ACS Appl. Opt. Mater.* **2023**, *1*, 906.
[23] D. E. Shen, A. M. Osterholm, J. R. Reynolds, *J. Mater. Chem. C* **2015**, *3*, 9715.
[24] M. Gugole, O. Olsson, K. Xiong, J. C. Blake, J. Montero Amenedo, I. Bayrak Pehlivan, G. A. Niklasson, A. Dahlin, *ACS Photonics* **2020**, *7*, 1762.
[25] M. Gugole, O. Olsson, V. K. Gupta, R. Bordes, E. Ahlberg, A. Martinelli, A. Dahlin, *ACS Appl. Opt. Mater.* **2023**, *1*, 558.
[26] M. Gugole, O. Olsson, S. Rossi, M. P. Jonsson, A. Dahlin, *Nano Lett.* **2021**, *21*, 4343.
[27] K. Xiong, G. Emilsson, A. Maziz, X. Yang, L. Shao, E. W. H. Jager, A. B. Dahlin, *Adv. Mater.* **2016**, *28*, 9956.
[28] S. Macher, M. Rumpel, M. Schott, U. Posset, G. A. Giffin, P. Lobmann, *ACS Appl. Mater. Interfaces* **2020**, *12*, 36695.
[29] I. D. Brotherston, Z. Cao, G. Thomas, P. Weglicki, J. R. Owen, *Sol. Energy Mater. Sol. Cells* **1995**, *39*, 257.
[30] P. M. M. C. Bressers, E. A. Meulenkamp, *J. Electrochem. Soc.* **1998**, *145*, 2225.
[31] R. B. Goldner, G. Foley, E. L. Goldner, P. Norton, K. Wong, T. Haas, G. Seward, R. Chapman, *Appl. Opt.* **1985**, *24*, 2283.
[32] M. Szekely, C. Mathieu, N. E. Moulayat, M. Herlem, H. Cachet, M. Keddam, H. Perrot, B. Fahys, B. Eid, E. Caillot, *J. Electroanal. Chem.* **1996**, *401*, 89.
[33] M. Szekely, B. Eid, E. Caillot, M. Herlem, A. Etcheberry, C. Mathieu, B. Fahys, *J. Electroanal. Chem.* **1995**, *391*, 69.
[34] A. B. Dahlin, R. Zahn, J. Voros, *Nanoscale* **2012**, *4*, 2339.
[35] D. Aurbach, M. Daroux, P. Faguy, E. Yeager, *J. Electroanal. Chem. Interfacial Electrochem.* **1991**, *297*, 225.
[36] O. V. Tripachev, E. A. Maleeva, M. R. Tarasevich, *Russ. J. Electrochem.* **2015**, *51*, 103.
[37] J. P. Vivek, N. Berry, G. Papageorgiou, R. J. Nichols, L. J. Hardwick, *J. Am. Chem. Soc.* **2016**, *138*, 3745.
[38] T. Liu, J. P. Vivek, E. W. Zhao, J. Lei, N. Garcia-Araez, C. P. Grey, *Chem. Rev.* **2020**, *120*, 6558.
[39] J. Lindberg, B. Wickman, M. Behm, A. Cornell, G. Lindbergh, *J. Electroanal. Chem.* **2017**, *797*, 1.
[40] C. O. Laoire, S. Mukerjee, K. M. Abraham, E. J. Plichta, M. A. Hendrickson, *J. Phys. Chem. C* **2009**, *113*, 20127.
[41] Y. Zhong, G. T. M. Nguyen, C. Plesse, F. Vidal, E. W. H. Jager, *ACS Appl. Mater. Interfaces* **2018**, *10*, 21601.
[42] V. Seshadri, J. Padilla, H. Bircan, B. Radmard, R. Draper, M. Wood, T. F. Otero, G. A. Sotzing, *Org. Electron.* **2007**, *8*, 367.
[43] R. Brooke, I. Petsagkourakis, S. Majee, O. Olsson, A. Dahlin, P. Andersson Ersman, *Macromol. Mater. Eng.* **2022**, *308*, 2200453.
[44] S. Rossi, O. Olsson, S. Chen, R. Shanker, D. Banerjee, A. Dahlin, M. P. Jonsson, *Adv. Mater.* **2021**, *33*, 2105004.